

## Crystallographic and Magnetic Properties of Nano-sized Nickel Substituted Cobalt Ferrites Synthesized by the Sol-gel Method

Won-Ok Choi, Jae-Gwang Lee, Byung-Sub Kang, and Kwang Pyo Chae\*

Nanotechnology Research Center, Department of Nano Science and Mechanical Engineering, Konkuk University, Chungju 380-701, Korea

(Received 13 December 2013, Received in final form 11 February 2014, Accepted 11 February 2014)

Nano-sized nickel substituted cobalt ferrite powders,  $\text{Ni}_x\text{Co}_{1-x}\text{Fe}_2\text{O}_4$  ( $0.0 \leq x \leq 1.0$ ), were fabricated by the sol-gel method, and their crystallographic and magnetic properties were studied. All the ferrite powders showed a single spinel structure, and behaved ferrimagnetically. When the nickel substitution was increased, the lattice constants and the sizes of particles of the ferrite powders decreased. The Mössbauer absorption spectra of  $\text{Ni}_x\text{Co}_{1-x}\text{Fe}_2\text{O}_4$  ferrite powders could be fitted with two six-line subspectra, which were assigned to a tetrahedral A-site and octahedral B-sites of a typical spinel crystal structure. The increase in values of the magnetic hyperfine fields indicated that the superexchange interaction was stronger, with the increased nickel concentration in  $\text{Ni}_x\text{Co}_{1-x}\text{Fe}_2\text{O}_4$ . This could be explained using the cation distribution, which can be written as,  $(\text{Co}_{0.28-0.28x}\text{Fe}_{0.72+0.28x})[\text{Ni}_x\text{Co}_{0.72-0.72x}\text{Fe}_{1.28-0.28x}]\text{O}_4$ . The two values of the saturation magnetization and the coercivity decreased, as the rate of nickel substitution was increased. These decreases could be explained using the cation distribution, the magnetic moment, and the magneto crystalline anisotropy constant of the substituted ions.

**Keywords :** nickel cobalt ferrite, sol-gel method, Mössbauer spectroscopy, cation distribution, saturation magnetization, coercivity

### Introduction

Nano phase spinel ferrites have attracted much attention, due to their technological importance in a variety of fields. Also, the substituted cobalt ferrites have been shown to be promising candidate materials for stress and torsion sensor application [1]. Cobalt ferrite,  $\text{CoFe}_2\text{O}_4$ , is a well-known hard magnetic material that has been studied in detail, due to its high coercivity (about 5.40 kOe), and moderate saturation magnetization (about 80 emu/g); as well as its remarkable chemical stability, and mechanical hardness [2, 3]. Cobalt ferrite is basically an inverse spinel, with which a corrected cation distribution becomes  $(\text{Co}_{0.1}\text{Fe}_{0.9})[\text{Co}_{0.9}\text{Fe}_{1.1}]\text{O}_4$ . The degree of inversion depends on the thermal history. On the other hand, nickel ferrite,  $\text{NiFe}_2\text{O}_4$ , is a typical soft magnetic material, and an inverse spinel, in which the tetrahedral A-sites are occupied by  $\text{Fe}^{3+}$  ions, and the octahedral B-sites by  $\text{Fe}^{3+}$  and  $\text{Ni}^{2+}$  ions [4, 5]. Among the ferrosinels the inverse spinel type is

particularly interesting, due to its high magnetocrystalline anisotropy, and unique magnetic structure. Ni-Co ferrites are highly resistive, and magnetostrictive. Recently, the structural, magnetic and magnetostrictive properties of Ni-Co ferrites have been studied [6-8].

The sol-gel method is known as a technique for the low temperature synthesis of glass, ceramics, and other materials, using the dip coating solution or spin coating process for thin film [9-11]. One of the advantages of using the sol-gel method is the lower annealing temperature, which enables smaller grained powders to be grown. These ultra-fine cobalt ferrite particles have been intensively investigated. The sol-gel method can provide multi-component oxide with a homogeneous composition, and it has been employed to prepare many high purity oxide powders and film, including some products with spinel-type structures.

To our knowledge, there have only been a few detailed studies on nano-sized nickel substituted cobalt ferrites synthesized via the sol-gel method. In this study, using the sol-gel method, we synthesized nano-sized nickel substituted cobalt ferrite powders  $\text{Ni}_x\text{Co}_{1-x}\text{Fe}_2\text{O}_4$ , ranging from  $x = 0.0$  to  $x = 1.0$  step 0.2; and studied the crystallographic and magnetic properties, by means of X-ray diffracto-

©The Korean Magnetism Society. All rights reserved.

\*Corresponding author: Tel: +82-43-840-3623

Fax: +82-43-851-6169, e-mail: kpchae@kku.ac.kr

metry (XRD), field emission scanning electron microscope (FESEM). Mössbauer spectroscopy, and vibrating sample magnetometry (VSM).

## 2. Experiment

The samples of the  $\text{Ni}_x\text{Co}_{1-x}\text{Fe}_2\text{O}_4$  ( $0.0 \leq x \leq 1.0$ ) ferrite were prepared by the sol-gel method. Measured amounts of  $\text{Co}(\text{CH}_3\text{CO}_2)_2 \cdot 4\text{H}_2\text{O}$ ,  $\text{Fe}(\text{NO}_3)_3 \cdot 9\text{H}_2\text{O}$ , and  $\text{N}_2\text{NiO}_4$  were first dissolved in 2-Methoxyethanol for 30-50 min, by means of an ultrasonic cleaner. The solution was refluxed at  $80^\circ\text{C}$  for 12 h, in order to gel, and dried at  $100^\circ\text{C}$  in a dry oven for 48 h. The samples of the dried powders were ground, and annealed at  $600^\circ\text{C}$  for 6 h.

To verify their purity, all samples were analyzed by an X-ray diffractometer, with  $\text{CuK}\alpha$  ( $1.54 \text{ \AA}$ ) radiation. The surface microstructure was observed, using FESEM at room temperature. The Mössbauer spectra of the powders were recorded with a  $^{57}\text{Co}$  source in a constant acceleration mode, to identify the magnetic phase of cobalt ferrite powders. The saturation magnetization and coercivity were determined by VSM.

## 3. Results and Discussion

X-ray diffraction patterns of  $\text{Ni}_x\text{Co}_{1-x}\text{Fe}_2\text{O}_4$  ( $0.0 \leq x \leq 1.0$ ) ferrite powders are shown in Fig. 1 [12]. The x-ray

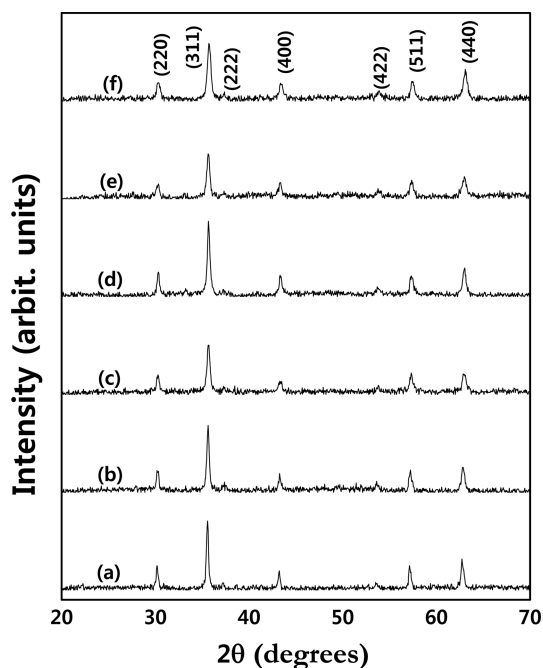


**Fig. 1.** X-ray diffraction patterns of  $\text{Ni}_x\text{Co}_{1-x}\text{Fe}_2\text{O}_4$  ferrites: (a)  $x = 0.0$ , (b)  $x = 0.2$ , (c)  $x = 0.4$ , (d)  $x = 0.6$ , (e)  $x = 0.8$ , and (f)  $x = 1.0$ .

diffraction measurement shows that all the peaks are consistent with those of a typical spinel structure of a cobalt ferrite powder, and no extra peaks were identified, corresponding to any secondary phase. The lattice constant of  $\text{Ni}_x\text{Co}_{1-x}\text{Fe}_2\text{O}_4$  ferrite powders linearly decreases from  $0.835 \text{ nm}$  at  $x = 0.0$ , to  $0.833 \text{ nm}$  at  $x = 1.0$ , with the nickel content. This can be explained by Vegard's law, which is that the larger  $\text{Co}^{2+}$  ( $0.074 \text{ nm}$ ) ions are substituted by the smaller  $\text{Ni}^{2+}$  ( $0.069 \text{ nm}$ ), which leads to decrease in the lattice constants. Similar results have been reported for Ni substituted cobalt ferrite nanoparticles [6].

The size of the particles was determined from the diffraction peak broadening with the use of the Scherrer equation [13],  $t = (0.9\lambda)/(B \cos \theta_B)$ , where  $\lambda$  represent the X-ray wavelength,  $B$  is the half width of the (311) peak, and  $\theta_B$  is the angle of the (311) peak. The particle size of our samples decreased, with increasing nickel concentration. The increase in the nickel concentration led to a broadening of the major peak, that is, a growth of the smaller particle size of our spinel powders, and improved crystallization. The particle size linearly decreased as  $25.9 \text{ nm}$  ( $x = 0.0$ ),  $25.0 \text{ nm}$  ( $x = 0.2$ ),  $22.1 \text{ nm}$  ( $x = 0.4$ ),  $21.0 \text{ nm}$  ( $x = 0.6$ ),  $18.5 \text{ nm}$  ( $x = 0.8$ ), and  $16.6 \text{ nm}$  ( $x = 1.0$ ). This suggests that the particle size of the nickel cobalt

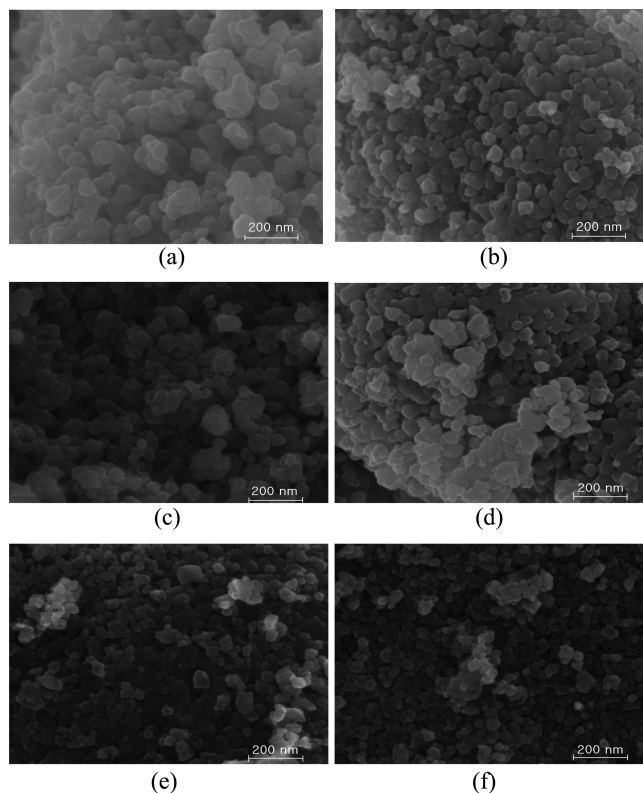


**Fig. 2.** SEM images ( $100,000\times$ ) of  $\text{Ni}_x\text{Co}_{1-x}\text{Fe}_2\text{O}_4$  ferrites: (a)  $x = 0.0$ , (b)  $x = 0.2$ , (c)  $x = 0.4$ , (d)  $x = 0.6$ , (e)  $x = 0.8$ , and (f)  $x = 1.0$ .

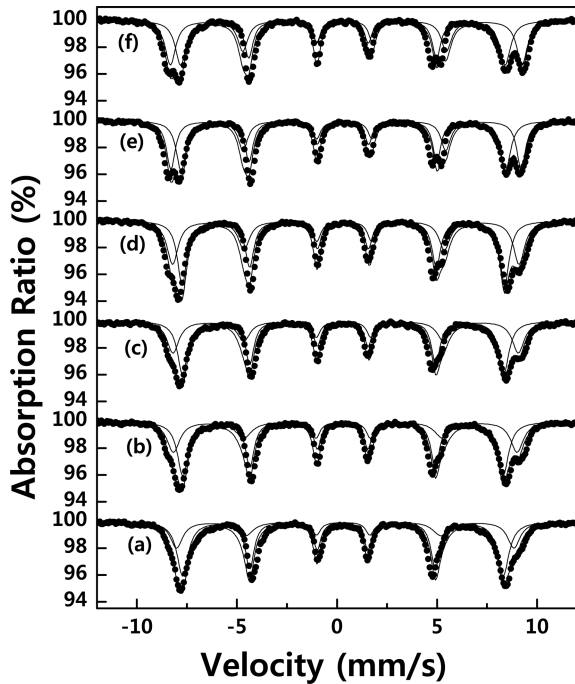


**Fig. 3.** Mössbauer spectra at room temperature of  $\text{Ni}_x\text{Co}_{1-x}\text{Fe}_2\text{O}_4$  ferrites: (a)  $x = 0.0$ , (b)  $x = 0.2$ , (c)  $x = 0.4$ , (d)  $x = 0.6$ , (e)  $x = 0.8$ , and (f)  $x = 1.0$ .

ferrites powder obtained through the sol-gel method is nano-size, and smaller, compared to that of powders obtained using the ceramic and wet chemical methods.

The decreasing of the grain sizes of  $\text{Ni}_x\text{Co}_{1-x}\text{Fe}_2\text{O}_4$  with increasing nickel concentration can be confirmed by FESEM at 100,000x magnification. All the samples have nearly homogeneous nano-size grains, as shown in Fig. 2. The average grain size determined from FESEM was noted as 63.9 nm ( $x = 0.0$ ), 51.0 nm ( $x = 0.2$ ), 50.2 nm ( $x = 0.4$ ), 41.7 nm ( $x = 0.6$ ), 38.6 nm ( $x = 0.8$ ), and 33.7 nm ( $x = 1.0$ ), which show that the grain size decreased, with increasing nickel substitution. It is known that the ferrite powders prepared by the ceramic method exhibit non uniform grain size distribution, with a grain size of greater than several  $\mu\text{m}$ .

The Mössbauer absorption spectra measured at room temperature for  $\text{Ni}_x\text{Co}_{1-x}\text{Fe}_2\text{O}_4$  ferrite powders are shown in Fig. 3 [12]. The spectra of all samples are fitted with two six-line subspectra, which are assigned to a tetrahedral A-site, and octahedral B-sites of a typical spinel crystal structure, as shown in Table 1. The values of quadruple splitting ( $QS$ ) and isomer shift ( $IS$ ) are almost unchanged with nickel concentration; whereas, those of magnetic hyperfine fields ( $H_{hf}$ ) are linearly increased in A- and B-sites. These values of Mössbauer parameter are in good agreement with those reported earlier for these ferrites

**Table 1.** Room temperature Mössbauer parameters of  $\text{Ni}_x\text{Co}_{1-x}\text{Fe}_2\text{O}_4$  ( $0.0 \leq x \leq 1.0$ ) ferrite powder.  $H_{hf}$  is the magnetic hyperfine field,  $QS$  is the quadrupole splitting, and  $IS$  represents the isomer shift relative to metallic iron, at room temperature.

x	$H_{hf}$ (kOe)		$QS$ (mm/s)		$IS$ (mm/s)	
	A-site	B-site	A-site	B-site	A-site	B-site
0.0	523.0	497.0	0.05	0.01	0.36	0.29
0.2	532.6	497.0	0.05	0.01	0.36	0.29
0.4	535.2	498.0	0.05	0.01	0.38	0.30
0.6	537.0	500.0	0.04	0.01	0.40	0.31
0.8	543.0	503.0	0.04	0.01	0.41	0.31
1.0	545.1	503.1	0.04	0.01	0.42	0.31

[14, 15]. The increasing of values of the magnetic hyperfine fields indicates that the superexchange interaction is stronger, with the nickel concentration in  $\text{Ni}_x\text{Co}_{1-x}\text{Fe}_2\text{O}_4$ . This can be explained, using the cation distribution. The cation distribution depends on many factors, such as temperature, pressure, and composition [16, 17]; as well as on the compound preparation method. Using the Mössbauer absorption area ratio of the A- and B-sites, and the occupation preference of Ni ions for B-sites in a spinel structure, we can determine the cation as  $(\text{Co}_{0.28-0.28x}\text{Fe}_{0.72+0.28x})[\text{Ni}_x\text{Co}_{0.72-0.72x}\text{Fe}_{1.28-0.28x}]\text{O}_4$ .

Using this cation distribution equation, we can explain the superexchange interaction being stronger with the

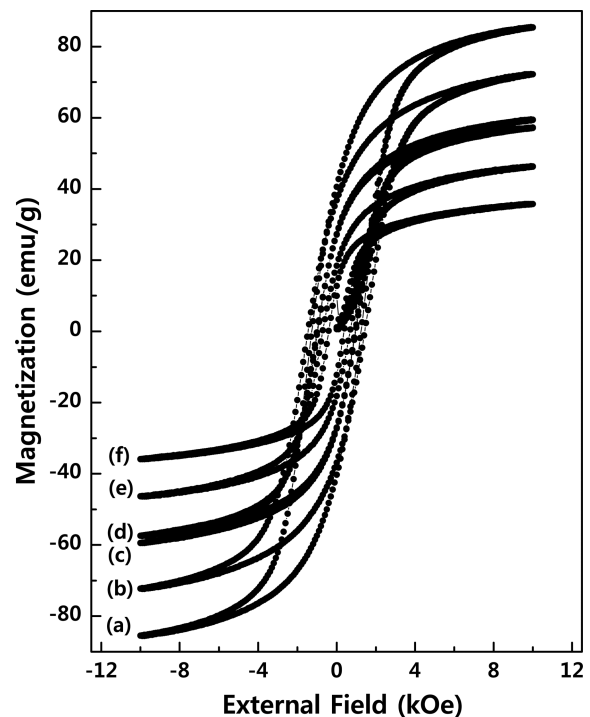


**Fig. 4.** Hysteresis curves of  $\text{Ni}_x\text{Co}_{1-x}\text{Fe}_2\text{O}_4$  ferrites: (a)  $x = 0.0$ , (b)  $x = 0.2$ , (c)  $x = 0.4$ , (d)  $x = 0.6$ , (e)  $x = 0.8$ , and (f)  $x = 1.0$ .

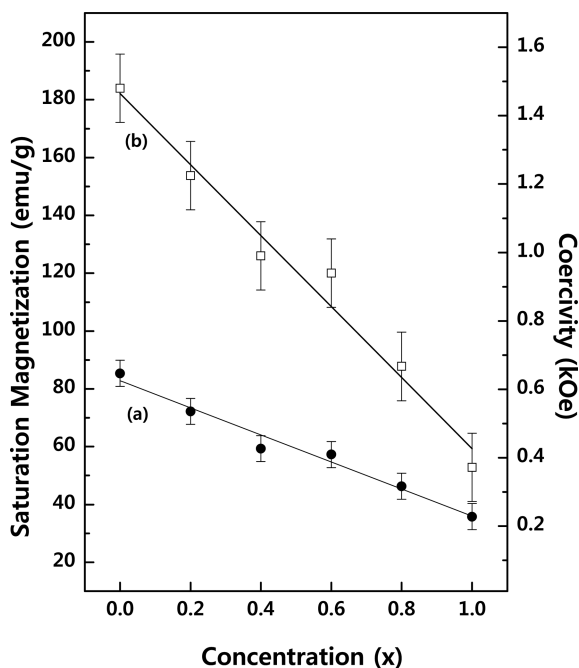


**Fig. 5.** Variation of the saturation magnetization and the coercivity of  $\text{Ni}_x\text{Co}_{1-x}\text{Fe}_2\text{O}_4$  ferrites: (a) saturation magnetization, and (b) coercivity.

nickel concentration. By increasing  $x$  until 1.0, the higher magnetic moment  $\text{Fe}^{3+}$  ions ( $5 u_B$ ) at A-sites increase, so the A-O-B superexchange becomes stronger in  $\text{Ni}_x\text{Co}_{1-x}\text{Fe}_2\text{O}_4$ ; although the lower magnetic moment  $\text{Co}^{2+}$  ( $3 u_B$ ) and  $\text{Ni}^{2+}$  ( $2 u_B$ ) ion's distribution are somewhat changed.

The magnetic properties of the  $\text{Ni}_x\text{Co}_{1-x}\text{Fe}_2\text{O}_4$  ( $0.0 \leq x \leq 1.0$ ) ferrite powders have been determined at room temperature, using VSM [12]. Fig. 4 shows the hysteresis curve, and Fig. 5 shows the changes of the saturation magnetization ( $M_s$ ) and the coercivity ( $H_c$ ), in the maximal field of 10 kOe. The values of  $M_s$  decrease linearly, with increasing nickel concentration. This decrease of  $M_s$  values can be explained by the smaller magnetic moment of  $\text{Ni}^{2+}$  ( $2 u_B$ ), as compared to the larger magnetic moment of  $\text{Co}^{2+}$  ( $3 u_B$ ). From the cation distribution equation, the  $\text{Fe}^{3+}$  ( $5 u_B$ ) distributed between A- and B-sites is almost unchanged, so the  $M_s$  values of  $\text{Ni}_x\text{Co}_{1-x}\text{Fe}_2\text{O}_4$  ferrites should be decreased, by increasing Ni concentration. The maximum value of  $M_s$  is 85.38 emu/g at  $x = 0.0$ , and the minimum value is 35.78 at  $x = 1.0$ . The coercivity also rapidly decreases linearly, with increasing nickel concentration. It is well known that the coercivity in polycrystalline ferrites strongly depends on the magneto crystalline anisotropy constant, and grain size. In our samples, the grain size did not change abruptly, so the main effect on coercivity decrease may be the lower magneto crystalline anisotropy constant of  $\text{Ni}^{2+}$ , with respect to that of  $\text{Co}^{2+}$ .

The maximum value of  $H_c$  is 1.48 kOe at  $x = 0.0$ , and the minimum value is 0.37 kOe at  $x = 1.0$ , respectively. From these results, we observe that the nickel substitute cobalt ferrites show lower coercivity and saturation magnetization, than pure cobalt ferrite powders.

## 4. Conclusion

The nickel substituted cobalt ferrites,  $\text{Ni}_x\text{Co}_{1-x}\text{Fe}_2\text{O}_4$  ( $0.0 \leq x \leq 1.0$ ), had a single spinel structure, and behaved ferrimagnetically. The lattice constants and the sizes of particles of the ferrite powders decreased, when the nickel substitution was increased. The Mössbauer absorption spectra measured at room temperature were fitted with two six-line subspectra, which are assigned a tetrahedral A-site and octahedral B-sites of a typical spinel crystal structure. The increasing of values of the magnetic hyperfine fields indicates that the superexchange interaction is stronger, with the nickel concentration in  $\text{Ni}_x\text{Co}_{1-x}\text{Fe}_2\text{O}_4$ . This could be explained, using the cation distribution. The cation distribution could be written as  $(\text{Co}_{0.28-0.28x}\text{Fe}_{0.72+0.28x})[\text{Ni}_x\text{Co}_{0.72-0.72x}\text{Fe}_{1.28-0.28x}]\text{O}_4$ . The magnetic behavior of ferrite powders showed that an increase in the nickel substitution yields a decrease in the saturation magnetization, and in the coercivity. The maximum saturation magnetization and the coercivity of  $\text{Ni}_x\text{Co}_{1-x}\text{Fe}_2\text{O}_4$  ferrite powders were 85.4 emu/g and 1,480 Oe, respectively, at  $x = 0.0$ . The minimum saturation magnetization and the coercivity of  $\text{Ni}_x\text{Co}_{1-x}\text{Fe}_2\text{O}_4$  ferrite powders were 35.8 emu/g and 370 Oe, respectively, at  $x = 1.0$ .

## Acknowledgements

This work was supported by Konkuk University.

## References

- [1] O. Caltun, H. Chiriac, N. Lupu, I. Dumitru, and B. A. Rao, *J. Optoelectro. Adv. Mater.* **9**, 1158 (2007).
- [2] N. N. Greenwood and T. C. Gibb, *Mössbauer Spectroscopy*, Chapman and Hall Ltd. London (1971), p. 261.
- [3] V. Blasko, V. Petkov, V. Rusanov, Ll. M. Martinez, B. Martinez, J. S. Muñoz, and M. Mikhove, *J. Magn. Magn. Mater.* **162**, 331 (1996).
- [4] A. S. Albaguerge, J. D. Ardisson, and W. A. A. Macedo, *J. Appl. Phys.* **87**, 4352 (2000).
- [5] A. Goldman, *Modern Ferrite Technology*, Van Nostrand Reinhold, New York (1990), p. 217.
- [6] M. Mozaffari, J. Amighian, and E. Darsheshdar, *J. Magn. Magn. Mater.* **350**, 19 (2014).
- [7] A. Ghasemi, A. P. Jr., and C. F. C. Machado, *J. Magn. Magn. Mater.* **324**, 2193 (2012).

- [8] V. L. Mathe and A. D. Sheikh, *Physica B* **405**, 3594 (2010).
- [9] J. G. Lee, J. Y. Park, and C. S. Kim, *J. Mater. Sci.* **53**, 3965 (1998).
- [10] V. K. Sankaranarayana, Q. A. Pankhurst, D. P. E. Dickson, and C. E. Johson, *J. Magn. Magn. Mater.* **125**, 199 (1993).
- [11] K. Oda, T. Yoshio, K. Hirata, K. O. Oka, and K. Takabashi, *J. Jpn. Soc. Powder Powder Metal.* **29**, 170 (1982).
- [12] W. O. Choi, Master thesis, Graduate School of Konkuk Univ. (2014).
- [13] B. D. Cullity, *Elements of X-Ray Diffraction*, Addison Wesley Co. (1978), p. 102.
- [14] C. V.-Aarca, P. Lavela, and J. L. Tirado, *J. Power Sources* **196**, 6978 (2011).
- [15] P. Didukh, J. M. Grenecheb, A.-S. Waniewska, P. C. Fannin, and L. Casas, *J. Magn. Magn. Mater.* **613**, 242 (2002).
- [16] M. Z. Schmalzrifd. *J. Phys. Chem.* **28**, 203 (1961).
- [17] R. K. Datta and B. Roy, *J. Amer. Coram. Soc.* **50**, 578 (1967).